

Structure of Neutron-Scattering Peak in both s_{++} -wave and s_{\pm} -wave states of an Iron pnictide Superconductor

Seiichiro ONARI¹, Hiroshi KONTANI², and Masatoshi SATO²

¹ *Department of Applied Physics, Nagoya University and JST, TRIP, Furo-cho, Nagoya 464-8602, Japan.*

² *Department of Physics, Nagoya University and JST, TRIP, Furo-cho, Nagoya 464-8602, Japan.*

(Dated: October 29, 2018)

We study the neutron scattering spectrum in iron pnictides based on the random-phase approximation in the five-orbital model, for fully-gapped s -wave states with sign reversal (s_{\pm}) and without sign reversal (s_{++}). In the s_{++} -wave state, we find that a prominent hump structure appears just above the spectral gap, by taking account of the quasiparticle damping γ due to strong electron-electron correlation: As the superconductivity develops, the reduction in γ gives rise to the large overshoot in the spectrum above the gap. The obtained hump structure looks similar to the resonance peak in the s_{\pm} -wave state, although the height and weight of the peak in the latter state is much larger. In the present study, experimentally observed broad spectral peak in iron pnictides is naturally reproduced by assuming the s_{++} -wave state.

PACS numbers: 74.20.-z, 74.20.Rp, 78.70.Nx

Since the discovery of superconductivity in iron pnictides with high transition temperature (T_c) next to high- T_c cuprates[1], the structure of the superconducting (SC) gap has been studied very intensively. The SC gap in many iron pnictides is fully-gapped and band-dependent, as shown by the penetration depth measurement [2] and the angle-resolved photoemission spectroscopy (ARPES) [3, 4], except for P-doped Ba122 [5]. The fully-gapped state is also supported by the rapid suppression in $1/T_1$ ($\propto T^n$; $n \sim 4 - 6$) below T_c [6–8].

In iron pnictides, the nesting of the Fermi surface (FS) between hole- and electron-pockets is expected to induce the antiferromagnetic (AF) fluctuations in doped metal compounds. Since fully-gapped sign-reversing s -wave state (s_{\pm} -wave state) is a natural candidate [9, 10], it is urgent to clarify the sign reversal in the SC gap via phase-sensitive experiments. One of the promising methods is the neutron scattering measurement: Existence of the resonance peak at a nesting wavevector \mathbf{Q} is a strong evidence for AF fluctuation mediated superconductors with sign reversal [11–13]. The resonance condition is $\omega_{\text{res}} < 2\Delta$, where ω_{res} is the resonance energy and Δ is magnitude of the SC gap at $T = 0$. The resonance peak has been observed in many AF fluctuation mediated unconventional superconductors, like high- T_c cuprates [14–16], CeCoIn₅ [17], and UPd₂Al₃ [18].

Neutron scattering measurements for iron pnictides have been performed [19–22] after the theoretical predictions [23, 24]. Although clear peak structure was observed in FeSe_{0.4}Te_{0.6} [20] and BaFe_{1.85}Co_{0.15}As₂ [21], its weight is much smaller than that in high- T_c cuprates and CeCoIn₅, and the resonance condition $\omega_{\text{res}} < 2\Delta$ is not surely confirmed, as we will discuss later.

Nonmagnetic impurity effect also offers us useful phase-sensitive information. Theoretically, s_{\pm} -wave state should be very fragile against impurities due to the inter-band scattering [25]; the predicted critical residual resis-

tivity $\rho_{\text{imp}}^{\text{cr}}$ for vanishing T_c is about $20 \mu\Omega\text{cm}$. However, experimental $\rho_{\text{imp}}^{\text{cr}}$ reaches $\sim 750 \mu\Omega\text{cm}$, which corresponds to the minimum metallic conductivity $4e^2/h$ per layer [26]. Since this result supports a conventional s -wave state without sign reversal (s_{++} -wave state), we have to resolve the discrepancy between neutron scattering measurements and the impurity effects.

In this letter, we study the dynamical spin susceptibility $\chi^s(\omega, \mathbf{Q})$ based on the five-orbital model [9] for both s_{++} and s_{\pm} wave states, and discuss by which pairing state the experimental results are reproducible. In the normal state, $\chi^s(\omega, \mathbf{Q})$ is strongly suppressed by the quasiparticle damping γ due to strong correlation. However, this suppression diminishes in the SC state since γ is reduced as the SC gap opens. For this reason, a prominent hump structure *unrelated to the resonance mechanism* appears in $\chi^s(\omega, \mathbf{Q})$ just above 2Δ in the s_{++} -wave state. In the s_{\pm} -wave state, very high and sharp resonance peak appears at $\omega_{\text{res}} < 2\Delta$. We demonstrate that the broad spectral peak observed in iron pnictides is naturally reproduced based on the s_{++} -wave state, rather than the s_{\pm} -wave state.

Now, we study the 10×10 Nambu BCS Hamiltonian $\hat{\mathcal{H}}_{\mathbf{k}}$ composed of the five-orbital tight-binding model and the band-diagonal SC gap introduced in ref. [25]. The FSs are shown in Fig. 1 (a). Then, the 10×10 Green function is given by

$$\begin{aligned} \hat{\mathcal{G}}(i\omega_n, \mathbf{k}) &\equiv \left(\begin{array}{cc} \hat{G}(i\omega_n, \mathbf{k}) & \hat{F}(i\omega_n, \mathbf{k}) \\ \hat{F}^\dagger(i\omega_n, \mathbf{k}) & -\hat{G}(-i\omega_n, \mathbf{k}) \end{array} \right)^{-1} \\ &= (i\omega_n \hat{1} - \hat{\Sigma}_{\mathbf{k}}(i\omega_n) - \hat{\mathcal{H}}_{\mathbf{k}})^{-1}, \end{aligned} \quad (1)$$

where $\omega_n = \pi T(2n + 1)$ is the fermion Matsubara frequency, \hat{G} (\hat{F}) is the 5×5 normal (anomalous) Green function, and $\hat{\Sigma}_{\mathbf{k}}$ is the self-energy in the d -orbital basis. For a while, we assume that the SC gap for the α -th FS is band-independent; $|\Delta_\alpha| = \Delta$. Hereafter, the unit of energy is eV, unless otherwise noted.

Here, we have to obtain the spin susceptibility as function of real frequency. For this purpose, it is rather easy to use the Matsubara frequency method and the numerical analytic continuation (pade approximation). In the present study, however, we perform the analytical continuation before numerical calculation in order to obtain more reliable results. The irreducible spin susceptibility in the singlet SC state is given by [13]

$$\hat{\chi}_{l_1 l_2, l_3 l_4}^{0R}(\omega, \mathbf{q}) = \frac{1}{N} \sum_{\mathbf{k}} \int \frac{dx}{2} \quad (2)$$

$$\left[\tanh \frac{x}{2T} G_{l_1 l_3}^R(x_+, \mathbf{k}_+) \rho_{l_4 l_2}^G(x, \mathbf{k}) \right. \\ + \tanh \frac{x}{2T} \rho_{l_1 l_3}^G(x_+, \mathbf{k}_+) G_{l_4 l_2}^A(x, \mathbf{k}) \\ + \tanh \frac{x}{2T} F_{l_1 l_4}^R(x_+, \mathbf{k}_+) \rho_{l_3 l_2}^{F\dagger}(x, \mathbf{k}) \\ \left. + \tanh \frac{x}{2T} \rho_{l_1 l_4}^F(x_+, \mathbf{k}_+) F_{l_3 l_2}^{\dagger A}(x, \mathbf{k}) \right],$$

where $x_+ = x + \omega$, $\mathbf{k}_+ = \mathbf{k} + \mathbf{q}$, $l_i = 1 \sim 5$ represents the d -orbital, and A (R) represents the advanced (retarded) Green function. $\rho_{ll'}^G(x, \mathbf{k}) \equiv (G_{ll'}^A(x, \mathbf{k}) - G_{ll'}^R(x, \mathbf{k})) / (2\pi i)$ and $\rho_{ll'}^{F(\dagger)}(x, \mathbf{k}) \equiv (F_{ll'}^{(\dagger)A}(x, \mathbf{k}) - F_{ll'}^{(\dagger)R}(x, \mathbf{k})) / (2\pi i)$ are one particle spectral functions. Since $\rho_{ll'}^{G,F}(x, \mathbf{k}) = 0$ for $|x| < \Delta$, $\text{Im} \hat{\chi}_{ll', l'' l'''}^{0R}(\omega, \mathbf{q}) = 0$ for $|\omega| < 2\Delta$. That is, the particle-hole excitation gap is 2Δ .

Then, the spin susceptibility $\chi^s(\omega, \mathbf{q})$ is given by the multiorbital random-phase-approximation (RPA) with the intraorbital Coulomb U , the interorbital Coulomb U' , the Hund coupling J , and the pair-hopping J' [9]:

$$\chi^s(\omega, \mathbf{q}) = \sum_{i,j} \left[\frac{\hat{\chi}^{0R}(\omega, \mathbf{q})}{1 - \hat{S}^0 \hat{\chi}^{0R}(\omega, \mathbf{q})} \right]_{ii, jj}, \quad (3)$$

where vertex of spin channel $\hat{S}_{l_1 l_2, l_3 l_4}^0 = U, U', J$ and J' for $l_1 = l_2 = l_3 = l_4$, $l_1 = l_3 \neq l_2 = l_4$, $l_1 = l_2 \neq l_3 = l_4$ and $l_1 = l_4 \neq l_2 = l_3$, respectively. Hereafter, we put $J = J' = 0.15$, $U' = U - 2J$, $U = 1 \sim 1.3$, and fix the electron number as 6.1 (10% electron-doped case). In the present model, $\chi^s(0, \mathbf{q})$ takes the maximum value when \mathbf{q} is the nesting vector $\mathbf{Q} = (\pi, \pi/16)$. Due to the nesting, $\chi^s(0, \mathbf{Q}) / \chi^0(0, \mathbf{Q}) \approx 1 / (1 - \alpha_{\text{St}})$ is enhanced; $\alpha_{\text{St}} (\lesssim 1)$ is the maximum eigenvalue of $\hat{S}^0 \hat{\chi}^{0R}(0, \mathbf{Q})$ that is called the Stoner factor.

In strongly correlated systems, $\chi^s(\omega, \mathbf{q})$ is renormalized by the self-energy correction. In nearly AF metals, for example, the temperature dependence of the self-energy induces the Curie-Weiss behavior of $\chi^s(0, \mathbf{Q})$. At the moment, there is no experimental information on the \mathbf{k} -, ϵ -, and band-dependences of the self-energy. Therefore, we phenomenologically introduce a band-diagonal self-energy as $\hat{\Sigma}_{\mathbf{k}}^R(\epsilon) = i\gamma(\epsilon)\hat{1}$. First, we estimate the value of $\gamma(\epsilon)$ in the normal state. Since the conductivity is given by $\sigma = e^2 \sum_{\alpha} N_{\alpha}(0) v_{\alpha}^2 / 2\gamma(0)$, where $N_{\alpha}(0)$ and v_{α} are the density of states (DOS) and the

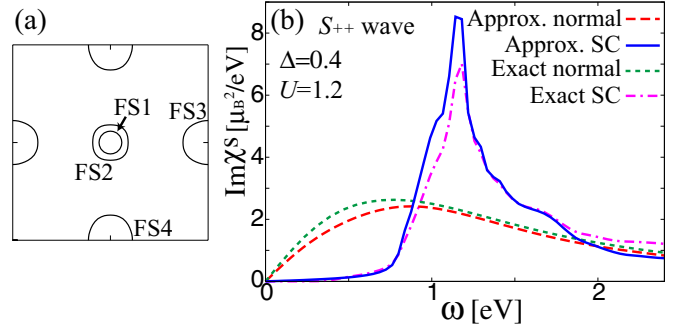


FIG. 1: (Color online) (a) FSs in iron pnictides. (b) ω -dependence of $\text{Im} \chi^s(\omega, \mathbf{Q})$ for the s_{++} -wave state ($\Delta = 0.4$) and the normal state, where the unit of energy is eV. The “exact result” is obtained by eq. (2), and the “approximate result” is obtained by eq. (6).

Fermi velocity of the α -th FS, we obtain $\rho \approx (2\gamma[\text{meV}]) \mu\Omega\text{cm}$ [25]. Since $\rho(T) - \rho(0) \sim (5T[\text{meV}]) \mu\Omega\text{cm}$ in $\text{BaFe}_{1.84}\text{Co}_{0.16}\text{As}_2$ below 100 K [27], $\gamma(0)$ due to inelastic scattering is estimated as $2.5T$ which is comparable to that in over-doped cuprates. If we assume the relation $\gamma(\epsilon) \propto (\pi T + \epsilon)$ in nearly AF Fermi liquid [28], we obtain $\gamma(\epsilon) \sim 2.5(T + \epsilon/\pi)$.

Now, we calculate $\text{Im} \chi^s(\omega, \mathbf{Q})$ in both normal and s_{++} -wave SC states, concentrating on the frequency $\omega \sim 2\Delta$. To estimate the renormalization of $\text{Im} \chi^s(\omega, \mathbf{Q})$ due to the self-energy, we have to know the value of $\gamma(\epsilon)$ with $|\epsilon| \sim \Delta$ in both normal and SC states. Considering that $\gamma(\epsilon) = 2.5(T + \epsilon/\pi) \sim 2\Delta$ at $T_c = 2.2$ meV and $\epsilon = \Delta \sim 5$ meV in $\text{BaFe}_{1.85}\text{Co}_{0.15}\text{As}_2$, in the present study, we simply put $\gamma(\epsilon)$ in the normal state at T_c as

$$\gamma(\epsilon) = \gamma_0 \quad (4)$$

with $\gamma_0 \gtrsim \Delta$. In the present model, $\alpha_{\text{St}} = 0.84$ (0.79) for $U = 1.3$ (1.2) when $\gamma_0 = 0.1$ and $T = 0.002$; the T -dependence of α_{St} is small when γ_0 is fixed.

In the SC state at $T \ll T_c$, $\gamma(\epsilon) = 0$ for $|\epsilon| < 3\Delta$ (= particle-hole excitation gap 2Δ plus one-particle gap Δ) [12], and its functional form is approximately the same as that in the normal state for $|\epsilon| \gtrsim 3\Delta$. Then, we put

$$\gamma(\epsilon) = a(\epsilon)\gamma_s \quad (5)$$

where (i) $a(\epsilon) \ll 1$ for $|\epsilon| < 3\Delta$, (ii) $a(\epsilon) = 1$ for $|\epsilon| > 4\Delta$, and (iii) linear extrapolation for $3\Delta < |\epsilon| < 4\Delta$. We have confirmed that the obtained results are insensitive to the boundary of $|\epsilon|$ (4Δ in the present case) between (ii) and (iii). Although γ_s at $T \ll T_c$ should be smaller than γ_0 at $T = T_c$, we simply put $\gamma_s = \gamma_0$ hereafter, which causes underestimation of the peak height of $\text{Im} \chi^s$.

Figure 1 shows $\text{Im} \chi^s(\omega, \mathbf{Q})$ obtained by eqs. (2) and (3) for $U = 1.2$, $\gamma_0 = 0.4$ and $T = 0.01$. In the s_{++} -wave SC state, we put $\Delta = \gamma_0$ and $a(3\Delta) = 0.05$. In calculating eq. (2), we use 256×256 \mathbf{k} -meshes, and

1000 x -meshes. Although values of Δ and γ in Fig. 1 are very large to obtain enough numerical accuracy, the ratio $\gamma_0/\Delta \sim 1$ is consistent with experiments. In the normal state, $\text{Im}\chi^s(\omega, \mathbf{Q})$ is suppressed by large quasiparticle damping $\gamma_0 \sim \Delta$. In the SC state, the gap in $\text{Im}\chi^s(\omega, \mathbf{Q})$ is 2Δ . Since the particle or hole with energy $|\epsilon| < 3\Delta$ is free from inelastic scattering in the SC state, the lifetime of particle-hole excitation with energy $|\epsilon| < 4\Delta$ becomes long. For this reason, $\text{Im}\chi^s(\omega, \mathbf{q})$ shows a large hump structure for $2\Delta \lesssim \omega \lesssim 4\Delta$ below T_c in s_{++} -wave state.

Unfortunately, we cannot put smaller Δ and γ in calculating eq. (2) in the five-orbital model, because of the computation time. To solve this problem, we perform the x -integration in eq. (2) approximately as follows: When $\hat{\gamma} = \gamma\hat{1}$, the retarded (advanced) 10×10 Green function is expressed as $\hat{G}_{m,m'}^{\text{R(A)}}(x, \mathbf{k}) = \sum_{\alpha} U_{\mathbf{k}}^{m,\alpha}(x + (-)i\gamma - E_{\mathbf{k}}^{\alpha})^{-1} U_{\mathbf{k}}^{m',\alpha*}$, where $E_{\mathbf{k}}^{\alpha}$ ($\alpha = 1 \sim 10$) is the eigenvalue of $\hat{\mathcal{H}}_{\mathbf{k}}$ and $\hat{U}_{\mathbf{k}}$ is the corresponding 10×10 unitary matrix. We promise that $E_{\mathbf{k}}^{\alpha} = -E_{\mathbf{k}}^{\alpha+5}$ for $1 \leq \alpha \leq 5$. When γ is sufficiently small, then $\rho_{ll'}^{\text{G(F)}}(x, \mathbf{k}) \approx \sum_{\alpha} U_{\mathbf{k}}^{l,\alpha} \delta(x - E_{\mathbf{k}}^{\alpha}) U_{\mathbf{k}}^{l'+5,\alpha*}$, and thus eq. (2) becomes

$$\hat{\chi}_{l_1 l_2, l_3 l_4}^{\text{0R}}(\omega, \mathbf{q}) \approx \frac{1}{N} \sum_{\mathbf{k}} \sum_{l, l'} \frac{f(E_{\mathbf{k}}^{l_1}) - f(E_{\mathbf{k}+\mathbf{q}}^{l_1'})}{\omega + E_{\mathbf{k}}^{l_1} - E_{\mathbf{k}+\mathbf{q}}^{l_1'} + i\Gamma_{ll', \mathbf{k}\mathbf{q}}} \left[U_{\mathbf{k}+\mathbf{q}}^{l_1, l_1'} U_{\mathbf{k}+\mathbf{q}}^{l_3, l_3'*} U_{\mathbf{k}}^{l_4 l_4'} U_{\mathbf{k}}^{l_2 l_2'*} + U_{\mathbf{k}+\mathbf{q}}^{l_1, l_1'} U_{\mathbf{k}+\mathbf{q}}^{l_4+5, l_4'*} U_{\mathbf{k}}^{l_3+5, l_3'} U_{\mathbf{k}}^{l_2 l_2'*} \right], \quad (6)$$

with $\Gamma_{ll', \mathbf{k}\mathbf{q}} = \gamma$ for $\gamma \ll 1$.

When γ is as large as Δ , however, we have to check to what extent eq. (6) is reliable. Considering that the origin of the renormalization of χ^s is the quasiparticle damping $\gamma(E_{\mathbf{k}}^{l_1})$ and $\gamma(E_{\mathbf{k}+\mathbf{q}}^{l_1'})$, we introduce the following approximation:

$$\Gamma_{ll', \mathbf{k}\mathbf{q}} = b \cdot \max\{\gamma(E_{\mathbf{k}}^{l_1}), \gamma(E_{\mathbf{k}+\mathbf{q}}^{l_1'})\} \quad (7)$$

where $b \approx 1$ is a fitting parameter. $\Gamma_{ll', \mathbf{k}\mathbf{q}} \approx 0$ in the SC state for $|E_{\mathbf{k}}^{l_1}|, |E_{\mathbf{k}+\mathbf{q}}^{l_1'}| < 3\Delta$, reflecting the absence of quasiparticle damping. In Fig. 1, we show numerical results given by the present approximation with $b = 1.3$; we replace $b\gamma_0$ with γ_0 hereafter since $b \approx 1$. Since the “exact results” given by eq. (2) is quantitatively reproduced, we decide to calculate $\text{Im}\chi^s(\omega, \mathbf{Q})$ using eqs. (6) and (7) for more realistic values of Δ and γ . We verified that the present approximation works well when γ is comparable to or smaller than Δ .

Figure 2 shows $\text{Im}\chi^s(\omega, \mathbf{Q})$ obtained by eqs. (6) and (3) for $U = 1.3$ and $T = 0.002$. In the s_{++} -wave SC state, we put $\Delta = 0.05$; although it is a few times larger than the gap for Sm1111 with $T_c = 56\text{K}$, it is enough smaller than the Fermi energies of electron- and hole-pockets [9]. In the numerical calculation, we use 1024×1024 \mathbf{k} -meshes. Hereafter, we put $a(3\Delta) = 0.003/\gamma_0$. When (a) $\gamma_0 = 0.003$, $\text{Im}\chi^s(\omega, \mathbf{Q})$ in the SC state approximately

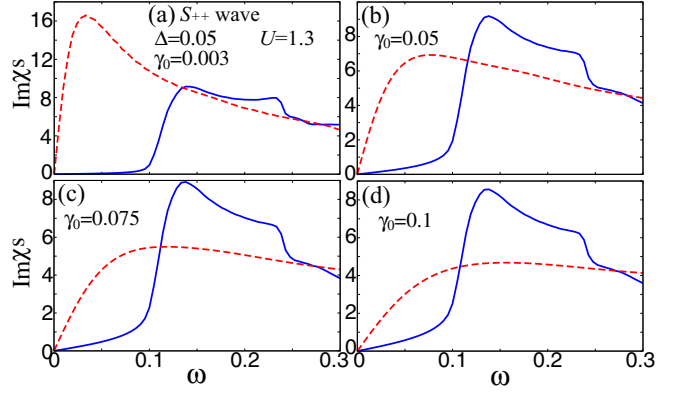


FIG. 2: (Color online) $\text{Im}\chi^s(\omega, \mathbf{Q})$ for s_{++} -wave (solid line) and normal (broken line) states, with $\gamma_0 = 0 \sim 0.1$.

equal to that in the normal state for $\omega > 2\Delta$. As γ_0 increases from (b) 0.05 to (d) 0.1, $\text{Im}\chi^s$ in the normal state decreases gradually, whereas that in the SC state depends on γ_0 only slightly, since $\gamma(\epsilon) \approx 0$ for $|\epsilon| < 3\Delta$. Therefore, in the case of $\gamma_0 \gtrsim \Delta$, $\text{Im}\chi^s(\omega, \mathbf{Q})$ in the SC state shows a prominent hump structure, and its peak value is about double of that in the normal state. In (d), experimental approximate “sum-rule” at fixed $\mathbf{q} = \mathbf{Q}$ [21] is well satisfied. In Fig. 2 (c) and (d), a relatively large slope for $|\epsilon| < 2\Delta$ is an artifact of the approximation due to large γ_0/Δ .

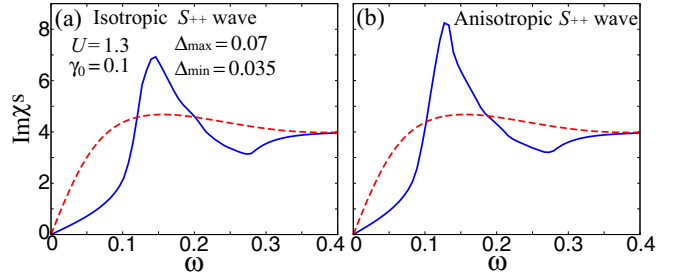


FIG. 3: (Color online) $\text{Im}\chi^s(\omega, \mathbf{Q})$ for s_{++} -wave (solid line) and normal (broken line) states, with $\Delta_{\text{max}} = 0.07$ and $\Delta_{\text{min}} = 0.035$.

Next, we study the effect of band-dependent SC gap observed by ARPES measurements [3, 4]. In Fig. 3 (a), we put $U = 1.3$, $\Delta_{1,2,4} = \Delta_{\text{max}} = 0.07\text{eV}$ for FS1,3,4, and $\Delta_2 = \Delta_{\text{min}} = 0.035\text{eV}$ for FS2. In (b), we introduce the anisotropy of the gap function for only FS3,4 with ratio 2; $\Delta_{\mathbf{k}} = \Delta_{\text{max}}(1 - 0.5 \sin^2 \theta_{\mathbf{k}})$, where $\theta_{\mathbf{k}} = \tan^{-1}(|k_{y(x)}|/(|k_{x(y)}| - \pi))$ for FS3(4). Here, we put $a(\epsilon)$ in eq. (5) as (i) $0.003/\gamma_0$ for $|\epsilon| < 3\Delta_{\text{min}}$, (ii) 1 for $|\epsilon| > 4\Delta_{\text{min}}$, and (iii) linear extrapolation for $3\Delta_{\text{min}} < |\epsilon| < 4\Delta_{\text{min}}$. In Fig. 3 (a), $\text{Im}\chi^s(\omega, \mathbf{Q})$ increases rapidly at $\omega = \Delta_{\text{max}} + \Delta_{\text{min}} = 0.105$, and it shows a peak at $\omega = 0.14$. In (b), the peak is located at $\omega = 0.125$, which is closer to $\Delta_{\text{max}} + \Delta_{\text{min}} = 0.105$. In Fig. 3 (a) and (b), the width of the hump peak is

much sharper than that for the band-independent SC gap in Fig. 2, since $\text{Im}\chi^s(\omega, \mathbf{Q})$ is reduced by damping for $|\omega| > 4\Delta_{\min} = 0.14$. We have also calculated $\text{Im}\chi^s(\omega, \mathbf{Q})$ for $\Delta_{3,4} = \Delta_{\max}$ and $\Delta_{1,2} = \Delta_{\min}$, and verified that the obtained result is similar to Fig. 3.

Here, we make comparison with experiments. The peak height and the weight in Fig. 3 (b) seems to be consistent with the neutron scattering measurements in iron pnictides [19–22]. In $\text{BaFe}_{1.85}\text{Co}_{0.15}\text{As}_2$ ($T_c = 25\text{K}$), the observed “resonance energy” is $\omega_{\text{res}} = 9.5$ meV [21]. According to ref. [3], $\Delta_{\max}/T_c \approx 3.5$ and $\Delta_{\min}/\Delta_{\max} \approx 0.35$ in many iron pnictides. (More smaller $\Delta_{\max,\min}$ is reported in ref. [2].) Thus, $\Delta_{\max} + \Delta_{\min} \approx 4.7T_c = 10$ meV is comparable to $\omega_{\text{res}} = 9.5$ meV in $\text{BaFe}_{1.85}\text{Co}_{0.15}\text{As}_2$. Moreover, finite $\text{Im}\chi^s(\omega, \mathbf{Q})$ for $\omega \gtrsim 0.3\omega_{\text{res}}$ in ref. [21] may suggest the existence of SC gap anisotropy. Therefore, the theoretical result in Fig. 3 (b) is well consistent with experimental data. We have verified that the hump structure of $\text{Im}\chi^s(\omega, \mathbf{q})$ with $\mathbf{q} = (\pi, 0)$ is very small for $\gamma_0 \sim 0.1$.

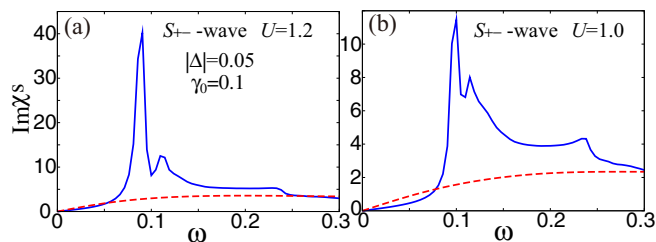


FIG. 4: (Color online) $\text{Im}\chi^s(\omega, \mathbf{Q})$ for s_{\pm} -wave (solid line) and normal (broken line) states, with $U = 1.2$ and 1.0 .

We also analyze the resonance peak for the s_{\pm} -wave state in Fig. 4. In this case, the spin wave without damping is observed as the “resonance peak” at $\omega_{\text{res}} < 2\Delta$. Figure 4 shows the numerical results for (a) $U = 1.2$ and (b) $U = 1.0$ in the case of $\Delta_{1,2} = -\Delta_{3,4} = 0.05$. In (a), a very sharp and high resonance peak appears at $\omega_{\text{res}} = 0.85 < 2\Delta$, consistently with previous theoretical studies [23, 24]. The case (b) with $U = 1.0$ corresponds to the “heavily overdoped” since $\alpha_{\text{St}} = 0.69$ and $T_c \sim 0$. The obtained resonance peak in Fig. 4 by taking $\gamma(\epsilon)$ into account is too large to explain experiments even in the case of $\alpha_{\text{St}} = 0.69$. In Bi-based high- T_c cuprates, the width of the resonance peak is wide due to the sample inhomogeneity (i.e., nanoscale distribution of T_c) [16]. However, weight of the peak is 10 times larger than that in $\text{BaFe}_{1.85}\text{Co}_{0.15}\text{As}_2$ [21].

In the present study, we have neglected the impurity effect since its influence on $\chi^s(\omega, \mathbf{Q})$ is expected to be small. In fact, in the single band model, the reduction in χ^0 due to the impurity self-energy is almost canceled by the impurity vertex correction [29]. Moreover, impurity effect tends to enhance $\chi^s(\omega, \mathbf{Q})$ in the modified FLEX approximation in nearly AF metals [30].

Before closing the study, we shortly discuss the heavy

fermion Kondo insulator CeNiSn . As shown in Fig. 1 of Ref. [31], neutron scattering spectrum at $\mathbf{q} = (0, \pi, 0)$ in CeNiSn shows a prominent hump peak structure above the hybridization gap below the Kondo temperature T_K , which looks very similar to the spectrum observed in iron pnictides below T_c [19–22]. This hump structure is well reproduced by the dynamical-mean-field theory based on the periodic Anderson model [32]. This fact demonstrates that large hump in $\text{Im}\chi^s(\omega, \mathbf{Q})$ can appear in strongly correlated systems with one-particle gap, without the necessity of the resonance mechanism.

In summary, we have studied $\text{Im}\chi^s(\omega, \mathbf{Q})$ in iron pnictides based on the five-orbital model, and revealed that a prominent hump structure appears just above 2Δ in the s_{++} -wave state, by taking the strongly correlation effect via γ . This hump structure becomes small as α_s decreases in the over-doped region or q deviates from the nesting. At present, experimental data can be explained in terms of the s_{++} -wave state very well. Further experimental efforts are required to determine the height and width of the “resonance peak”, and the magnitude relation between ω_{res} and $\Delta_{\max} + \Delta_{\min}$.

This study has been supported by Grants-in-Aid for Scientific Research from MEXT of Japan, and by JST, TRIP. Numerical calculations were performed using the facilities of the supercomputer center, ISSP.

- [1] Y. Kamihara, *et al.*, J. Am. Chem. Soc. **130**, 3296 (2008).
- [2] K. Hashimoto *et al.*, Phys. Rev. Lett. **102**, 017002 (2009).
- [3] D. V. Evtushinsky *et al.*, New J. Phys. **11**, 055069 (2009).
- [4] K. Nakayama *et al.*, Europhys. Lett. **85**, 67002 (2009).
- [5] K. Hashimoto *et al.*, arXiv:0907.4399.
- [6] Y. Kobayashi *et al.*, J. Phys. Soc. Jpn. **78** (2009) 073704.
- [7] H. Mukuda *et al.*, J. Phys. Soc. Jpn. **77**, 093704 (2008).
- [8] G. Fuchs *et al.*, arXiv:0908.2101.
- [9] K. Kuroki *et al.*, Phys. Rev. Lett. **101**, 087004 (2008); K. Kuroki *et al.*, Phys. Rev. B **79**, 224511 (2009).
- [10] I. I. Mazin *et al.*, Phys. Rev. Lett. **101**, 057003 (2008).
- [11] D. K. Morr and D. Pines, Phys. Rev. Lett. **81**, 1086 (1998).
- [12] A. Abanov and A. V. Chubukov, Phys. Rev. Lett. **83**, 1652 (1999).
- [13] T. Takimoto and T. Moriya, J. Phys. Soc. Jpn. **67**, 3570 (1998).
- [14] S. Iikubo, *et al.*, J. Phys. Soc. Jpn. **74**, 275 (2005).
- [15] M. Ito, *et al.*, J. Phys. Soc. Jpn. **71**, 265 (2002).
- [16] H. F. Fong, *et al.*, Nature **398**, 588 (1999).
- [17] C. Stock, *et al.*, Phys. Rev. Lett. **100**, 087001 (2008).
- [18] N. K. Sato, *et al.*, Nature **410**, 340 (2001).
- [19] A. D. Christianson, *et al.*, Nature **456**, 930 (2008).
- [20] Y. Qiu, *et al.*, Phys. Rev. Lett. **103**, 067008 (2009).
- [21] D. S. Inosov, *et al.*, arXiv:0907.3632.
- [22] J. Zhao, *et al.*, arXiv:0908.0954.
- [23] T. A. Maier and D. J. Scalapino, Phys. Rev. B **78**, 020514(R) (2008); T. A. Maier *et al.*, Phys. Rev. B **79**, 224510 (2009).
- [24] M. M. Korshunov and I. Eremin, Phys. Rev. B **78**,

- 140509(R) (2008).
- [25] S. Onari and H. Kontani, Phys. Rev. Lett. **103** (2009) 177001.
- [26] M. Sato *et al.*, arXiv:0907.3007.
- [27] A.S. Sefat *et al.*, arXiv:0903.0629.
- [28] B. P. Stojkovic and D. Pines, Phys. Rev. B **56**, 11931 (1997).
- [29] N. Bulut, Physica C, **353**, 270 (2001).
- [30] H. Kontani, Rep. Prog. Phys. **71**, 026501 (2007).
- [31] H. Kadowaki *et al.*, J. Phys. Soc. Jpn. **63**, 2074 (1994).
- [32] T. Mutou and D. S. Hirashima, J. Phys. Soc. Jpn. **64**, 4799 (1997).